Journal of Engineering Physics and Thermophysics, Vol. 82, No. 2, 2009

HEAT AND MASS TRANSFER IN DISPERSION AND POROUS MEDIA

GASIFICATION OF BELARUSIAN OIL SHALES IN A FILTRATION-COMBUSTION WAVE

K. V. Dobrego, S. A. Zhdanok, and I. A. Koznacheev

UDC 536.46

The regimes of gasification of Belarusian oil shales have been analyzed based on a generalized volume-averaged filtration-combustion model. The existence of three basic regimes — those of cocurrent and countercurrent filtration waves and of low-temperature volume pyrolysis — has been established. Data on the conditions of their existence have been obtained. The heat content of a producer gas in shale gasification in a stationary cocurrent filtration-combustion wave with air and oxygen-enriched blast has been evaluated.

Keywords: *oil shales, filtration combustion, gasification, mathematical simulation.*

Introduction. Oil (combustible) shales are sedimentary carbonate, silica, or clay rocks containing 15 to 40% of the organic matter, i.e., kerogen, from which liquid or gaseous hydrocarbon products can be obtained. We know of oil-shale deposits on all the continents; world shale reserves are estimated at $6.5 \cdot 10^{13}$ tons. In Belarus, shales are mainly concentrated in the Pripyat' shale basin of area above 20,000 km^2, forecast reserves 8.8 billion tons, and real commercial reserves 3.6 billion tons [1]. The prospects for utilizing Belarusian shales have been investigated in the 1970s [2]; however due to the change in the economic conditions and gradual depletion of traditional fuel and energy resources these issues become topical again.

Utilization of shales as a direct fuel is limited because of the difficulty of ash removal and ash collection, related environmental problems, etc. The Estonian and Baltic hydroelectric stations and the Ahtme and Kohtla-Yärve heat and electric power plants burn Baltic shales. BKZ-75 boilers (Syzran' thermal electric power plant) have long burned shales of the Kashpirskoe field with fuel-oil lighting. One of the best shale-processing technologies today is thermal extraction of shale gum and volatiles on UTT-3000 solid-heat-carrier units of shale output 139 tons/h. Its advantage is the possibility of processing low-grade shales [3, 4].

Due to the low calorific value of Belarusian shales (the heat of combustion is approximately 5.8 MJ/kg) it seems important to investigate progressive technologies of their gasification, in particular, with the use of nonstationary filtration combustion (FC) for controlling temperature regimes [5]. The issues of gasification of hydrocarbon raw material have been the focus of [6–8]; therefore, the procedure and methods of gasification are not discussed in the present work.

There are no experimental data on the FC of Belarusian shales and their gasification in the literature at present. The processes of FC and gasification of other fuels with a low content of organic matter have been considered in [9, 10]. It has been shown that the organic matter can burn out both completely and incompletely.

Realization of countercurrent regimes of propagation of an FC wave requires a fairly calorific fuel, since the maximum temperature in the system is lower than the adiabatic temperature of combustion of the fuel in this case [5]. Therefore, oxidation of Belarusian shales in a countercurrent wave requires an oxygen blast or the addition of a high-calorific fuel gas to the blast. On the other hand, the velocity of propagation of a countercurrent wave is much lower, as a rule, than the velocity of a cocurrent FC wave; consequently, the gasification productivity is lower. Thus, gasification in a cocurrent FC wave may be reckoned as a more acceptable process in terms of technology and economics.

A. V. Luikov Heat and Mass Transfer Institute, National Academy of Sciences of Belarus, 15 P. Brovka Str., Minsk, 220072, Belarus. Translated from Inzhenerno-Fizicheskii Zhurnal, Vol. 82, No. 2, pp. 205–214, March–April, 2009. Original article submitted March 18, 2008.

1062-0125/09/8202-0199

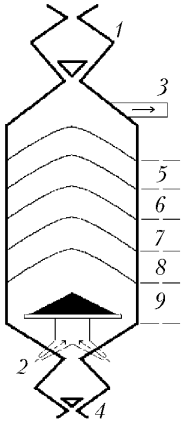

Fig. 1. Basic processes occurring in gasification of a hydrocarbon raw material in the direct-type reactor: 1) raw-material feed; 2) blast feed; 3) escape of the producer gas; 4) outlet of the ash; 5) drying (300–400 K); 6) pyrolysis (400–1000 K); 7) gasification (1000–1500 K); 8) combustion (1000–2000 K); 9) cooling of the ash, heating of the gas (400–600 K).

In the present work, we identify possible regimes of FC of a one-dimensional shale bed. For the regime of cocurrent propagation of an FC wave (gasification), we evaluate the parameter of the greatest practical importance, i.e., the calorific value of a producer gas in the case of an air and oxygen-enriched blast. The obtained data are basic for evaluation of the prospects for utilizing Belarusian shales as a raw material for gas-producing units.

Formulation of the Problem. We consider a heat-insulated cylindrical reactor (length L and a diameter d) filled with ground oil shales. The radial distribution of the parameters in the reactor is disregarded (one-dimensional approximation). To evaluate the qualitative features of FC we consider a closed reactor (without shale feeding and ash waste). In shale gasification in a stationary regime, the shale is continuously fed to the reactor and the ash is collected, which ensures the establishment of temperature and concentration fields. Firing is carried out by assigning a high-temperature region at the initial instant of time.

The basic processes in gasification of a hydrocarbon raw material are schematized in Fig. 1.

For investigation, we use a generalized volume-averaged model [11] within whose framework we make the following assumptions: a two-phase system (gas–solid phase) is considered; equations for the gas phase are written per unit volume of the gas phase; the equation of energy transfer in the solid phase is written per unit volume of the entire system; the porosity is constant throughout the reactor volume; the solid-phase density, not the particle size, changes in pyrolysis; in combustion of carbon, the particle size diminishes until it reaches the smallest size corresponding to that of an ash particle; particles settle instantaneously with decrease in their size; in continuous operation of the reactor, shale is fed continuously with a constant rate; the influence of the solid-phase motion on the heat exchange and hydrodynamics in the gas phase is disregarded.

Basic Equations. The system is described by the equations of continuity, motion, and energy for the gas, the mass equation for the gas components, and the energy and mass equation for the solid phase

$$\frac{\partial \rho_g}{\partial t} = -\frac{\partial (\rho_g u_g)}{\partial x} + \sum_i R_i ; \tag{1}$$

$$\rho_g \frac{\partial u_g}{\partial t} = -\rho_g u_g \frac{\partial u_g}{\partial x} - \frac{\partial p}{\partial x} + f, \quad f = -\frac{\mu}{k_0} u_g - \frac{\rho_g}{k_1} |u_g| u_g ; \tag{2}$$

$$\rho_g \frac{\partial c_i}{\partial t} = -\rho_g u_g \frac{\partial c_i}{\partial x} - \frac{\partial I_i}{\partial x} + R_i - c_i \sum_j R_j , \quad I_i = -\rho_g D_{\text{dis}} \frac{\partial c_i}{\partial x} ; \tag{3}$$

$$\rho_g c_{pg} \frac{\partial T_g}{\partial t} + \rho_g c_{pg} u_g \frac{\partial T_g}{\partial x} = -\frac{\partial J}{\partial x} + \frac{\alpha}{\varepsilon}(T_s - T_g) + Q_g, \quad J = -\lambda_{dis} \frac{\partial T_g}{\partial x}; \tag{4}$$

$$(1-\varepsilon)\frac{\partial (\rho_s c_{ps} T_s)}{\partial t} = \frac{\partial}{\partial x}\left(\lambda_{eff} \frac{\partial T_s}{\partial x}\right) + \alpha (T_g - T_s) + Q_s; \tag{5}$$

$$\frac{\partial d_p}{\partial t} + u_p \frac{\partial d_p}{\partial x} = -\frac{w_C d_p}{3\chi\rho_{r0}}. \tag{6}$$

The gas velocity u_g is related to the Darcy filtration velocity V_g by the equality $V_g = \varepsilon u_g$.

We consider three components of the solid phase: kerogen, carbon, and inert ash, for which we write the mass equations

$$\frac{\partial \rho_r}{\partial t} + u_p \frac{\partial \rho_r}{\partial x} = w_C \frac{\rho_r}{\chi\rho_{r0}} - w_r, \tag{7}$$

$$\frac{\partial \rho_C}{\partial t} + u_p \frac{\partial \rho_C}{\partial x} = w_C \frac{\rho_C}{\chi\rho_{r0}} - w_C + \chi w_r, \tag{8}$$

$$\frac{\partial \rho_a}{\partial t} + u_p \frac{\partial \rho_a}{\partial x} = w_C \frac{\rho_a}{\chi\rho_{r0}}. \tag{9}$$

The velocity of the bed of solid-phase particles is determined from the equation

$$\frac{\partial u_p}{\partial x} = -\frac{w_C}{\chi\rho_{r0}}. \tag{10}$$

The rate of heat release in the gas (per unit volume of the gas phase) is

$$Q_g = -\sum_i h_i R_{gi}, \tag{11}$$

where R_{gi} is the rate of formation of the components in *gas-phase* reactions. The rate of heat release in the solid phase (per unit volume of the entire system) is

$$Q_s = -\varepsilon \sum_i h_i R_{hi} - \varepsilon \sum_l h_l R_{hl}, \tag{12}$$

where R_{hi} and R_{hl} are the rates of formation of the components in *heterogeneous* reactions.

The values of the effective coefficients of transfer in the solid phase are computed from the empirical formulas given in [5, 11]. The molar heat capacities and enthalpies of the components of the gas mixture are calculated from the polynomial formulas of the CHEMKIN thermodynamic database [12]. The coefficients of diffusion, viscosity, and thermal conductivity of the gas mixture are approximated by the corresponding coefficients for nitrogen (in SI units): $D_g = 10^{-4} T_g^{1.75}/p$, $\mu = 4.4 \cdot 10^{-7} T_g^{0.65}$, $\lambda_g = 1.4\cdot 10^{-2} + 4.8\cdot 10^{-5} T_g$ (the characteristic error is 3%).

Chemical-Kinetics Model. We consider nine components of the gas phase: CO, CO_2, H_2, N_2, CH_4, H_2O, O_2, and H and OH radicals. The initial composition of the shales (the data have been taken from [2]) is as follows: the organic matter is 18 wt. % and the ash is 82 wt. %. The evaporation of moisture and the yield of constitution

(pyrogenetic) moisture from the shale are disregarded. A steam, just as solid carbon (coke), is formed in the process of pyrolysis according to the balance formula

$$1 \text{ kg of kerogen} \rightarrow 820 \text{ g C} + 56.8 \text{ g } CO_2 + 30.1 \text{ g CO} + 23 \text{ g } CH_4 + 1.8 \text{ g } H_2 + 8.3 \text{ g } N_2 + 60 \text{ g } H_2O \,. \tag{13}$$

The oxidation of carbon is described by the heterogeneous reactions [13]

$$C + O_2 = CO_2 \,, \tag{14}$$

$$CO_2 + C = 2CO \,. \tag{15}$$

The processes in the gas phase are described by the gross model proposed in [14].

The rate of formation of the jth component of the gas phase is expressed by the formula

$$R_j = \sum_k s_{jk} K_k \prod_i Y_i^{P_{ik}} \prod_l S_l^{P_{lk}} \,. \tag{16}$$

Summation is over all the chemical reactions involving the jth component of the gas mixture. The rate constant of each reaction is represented by the Arrhenius formula

$$K_k = z_k T^{P_{Tk}} \exp\left(-\frac{E_k}{T}\right). \tag{17}$$

We use temperature T_g for the gas-phase reactions and T_s for the heterogeneous reactions in calculating.

Boundary Conditions and Computational Procedure. The initial temperature distribution is assigned by a step function:

$$T_g = T_0 \,, \quad T_s = \begin{cases} T_b \,, & \text{for } x_{b.lt} < x < x_{b.r} \,, \\ T_0 \,, & \text{for } x \ge x_{b.r} \text{ and } x \le x_{b.lt} \,. \end{cases}$$

The inlet temperature of the gas is $T_g\big|_{x=0} = T_0$. Heat exchange of the gas with the porous medium at the boundary of the computational domain is absent; heat conduction is set equal to zero: $\left.\frac{\partial T_g}{\partial x}\right|_{x=0} = \left.\frac{\partial T_g}{\partial x}\right|_{x=L} = 0$. The system exchanges heat with the environment by radiation (gray body). The environmental temperature is T_0 on the inlet cross section and T_{ext} at exit.

A constant flow rate G and a composition of the blast c_i are assigned at entry, whereas a fixed particle size and partial densities of the solid-phase components are assigned at exit.

Simulation is carried out using a modified 2DBurner program [15] developed at the Heat and Mass Transfer Institute of the National Academy of Sciences of Belarus. The problem is solved on a uniform grid. We use the algorithm optimized for this system of rigorous nonlinear differential equations. On obtaining all data on the ith time layer the diffusion equation for the components (3) is discretized by the implicit scheme simultaneously with the chemical kinetic equations and are integrated by the Newton method. Thereafter Eqs. (5) and (6) are simultaneously integrated by the same method. From Eqs. (1) and (2), we derive a Poisson-type equation for pressure on the ith + 1 time layer (modified analog of the MAK method [16]), which is solved by the conjugate-gradient method or by the method of fast Fourier transformation [17, 18]. The velocity field is calculated in terms of the pressure field. In [19], we have verified the above model and algorithm; the verification was based on a comparison of the calculated and experimental temperatures in the reactor of oxidation of a lean mixture at the nonstationary stage of its startup.

Nonstationary Regimes of FC of Shales. Oil shales are of a low heat content, just as brown coal whose gasification regimes have qualitatively been described in [9]. A distinctive feature of the gasification of shales compared to the gasification of brown coal is the absence of the regime of slow low-temperature volume gasification,

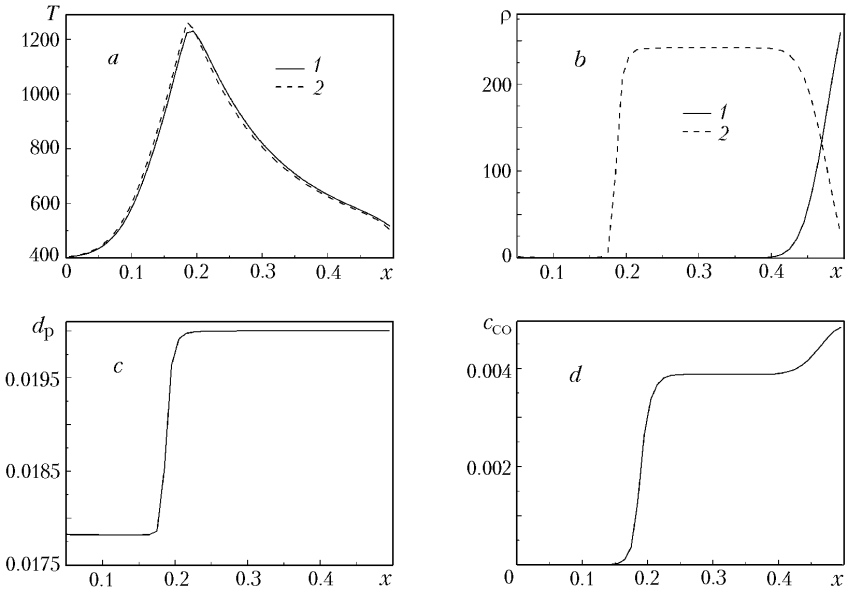

Fig. 2. Cocurrent gasification wave. The profiles of: a) temperatures of the gas T_g (1) and solid T_s (2) phases, b) partial densities in the solid phase of kerogen ρ_r (1) and carbon ρ_C (2), c) particle size d_p, and d) weight fraction of carbon monoxide c_{CO}. T_g and T_s, K; ρ_r and ρ_C, kg/m^3; d_p, m.

which is due to the high energy of activation of carbon oxidation (at temperatures of the order of 700 K or lower, we have a slow low-temperature pyrolysis, not the reactions of carbon oxidation).

We consider the qualitative features of FC in a closed reactor for the following standard values of the parameters:

Reactor length	0.5 m
Reactor-tube diameter	0.5 m
Firing region	$0 < x < 0.1$ m
Initial temperature of the system (except for the firing region)	400 K
Temperature of the environment and the blast	400 K
Firing temperature	1000 K
Composition of the blast:	
O_2	20 vol. %
N_2	80 vol. %
Flow rate of the blast (under normal conditions)	10 m^3/h
Specific flow rate of the blast (under normal conditions)	50.92 m^3/(m^2·h)
Specific mass flow rate of the blast	65.5 kg/(m^2·h)
Initial density of the solid-phase substance	1640 kg/m^3
Porosity of the shale fill	10%
Initial size of raw-material particles	0.02 m
Thermal conductivity of the shale bed	0.8 W/(m·K)
Heat capacity of the shale substance	1000 J/(kg·K)
Emissivity factor of the walls	0.45

A cocurrent gasification wave is formed at firing temperatures higher than 800 K in both firing/heating throughout the gasifier volume and firing near the gasifier inlet. Figure 2 gives the typical profiles of temperatures of the gas T_g and solid T_s phases, partial densities of the initial fuel substance ρ_r and carbon ρ_C in the solid phase, particle size d_p and weight fraction of CO in the gas phase c_{CO} for this regime.

A countercurrent gasification wave is formed under the same conditions in firing near the gasifier outlet. The typical profiles for this regime are shown in Fig. 3. One of the humps of the carbon density in Fig. 3b is related to

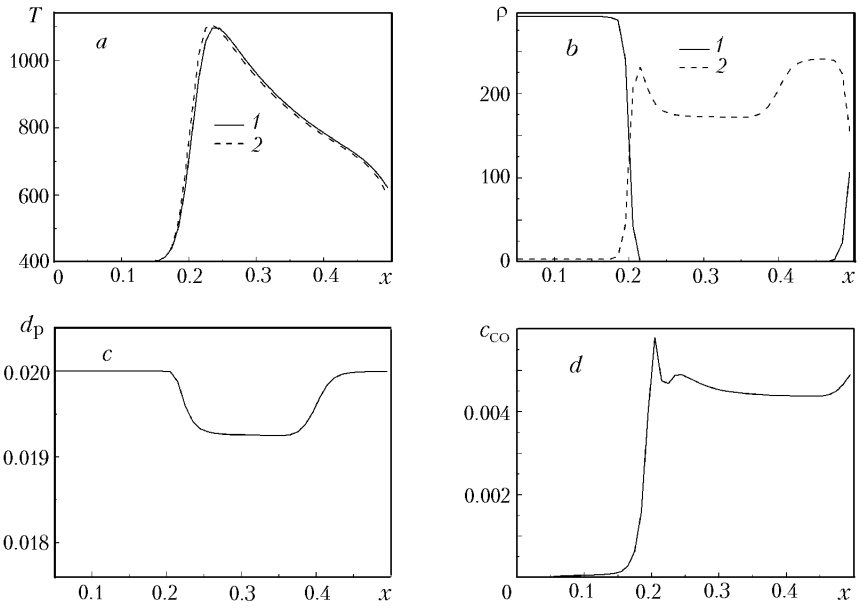

Fig. 3. Countercurrent gasification wave. The notation is the same as that in Fig. 2.

the region of primary heating in firing, since the process of oxidation began at the left-hand boundary of the hot region (and next propagated to the left) and the entire oxygen was expended before the traversal of this high-temperature region by the gas. The second small hump is in the region of the combustion front and corresponds to the carbon that has been produced from kerogen and has not managed to oxidize. The peak of the CO concentration in Fig. 3d is related to the fast kinetics of oxidation at the maximum temperature and to the shift of equilibrium in the CO–CO_2 system toward CO.

A distinctive feature of this regime is that a cocurrent carbon-reburning wave in whose propagation carbon is reburned virtually completely is formed at the gasifier inlet on transmission of the countercurrent wave.

Thus, as in the case of the gasification of lean coal beds, the regime of gasification in the cocurrent combustion wave is characterized by the oxidation of the entire carbon of the solid phase, and only part of the carbon is oxidized in the countercurrent-wave regime.

In firing, at the center of the gasifier, a cocurrent pyrolysis wave propagating toward the gasifier outlet and a countercurrent gasification wave propagating to the inlet are formed simultaneously. The typical temperature and partial-density profiles for such a regime are shown in Fig. 4.

An analog of the regime of low-temperature volume gasification [9] is the regime of low-temperature pyrolysis throughout the gasifier volume. It occurs when the firing temperature is sufficiently high for pyrolysis but insufficient for oxidation of the gaseous pyrolysis products and carbon. The typical profiles for this regime are shown in Fig. 5. The evolution of such a regime is reduced to the fact that the pyrolysis slows down and becomes "frozen" due to the gradual cooling of the reactor because of the heat loss through the walls. Carbon is hardly expended in this case.

Stationary Gasification. To simulate the stationary gasification regime we allow for the continuous removal of ash. For this purpose we introduce the velocity of displacement of the ash bed; the displacement velocity is selected so that the position of the gasification front in the system is constant and corresponds to the coordinate $x = 0.1$ m.

A temperature difference is formed in the reactor in gasification, and the gasification and pyrolysis regions are spatially separated (Figs. 2 and 3). The mixture of pyrolysis gases and gasification products forms a producer gas. If we abstract from a detailed composition of the producer gas (number of condensable fractions, etc.), we investigate its heating power as a function of the time, the flow rate of an air blast, and the concentration of oxygen in the blast.

Let us calculate the time evolution of the specific heat content of the producer gas after firing in the case of a closed reactor and a reactor with a continuously fed fuel (Fig. 6). The first portion of the curves in Fig. 6 (to 1 sec) is related to the traversal of the pyrolysis products to the reactor outlet; the time period 1–100 sec corresponds to the propagation of a pyrolysis wave; the gasification of the carbon residue occurs in the time interval 100–100,000 sec. A

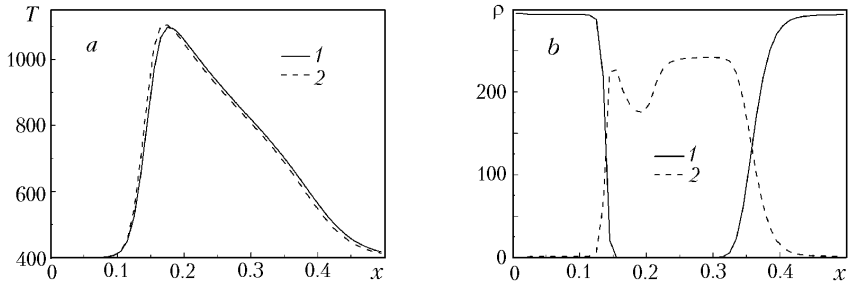

Fig. 4. Cocurrent and countercurrent waves in firing at the center of the gasifier. The notation is the same as that in Fig. 2.

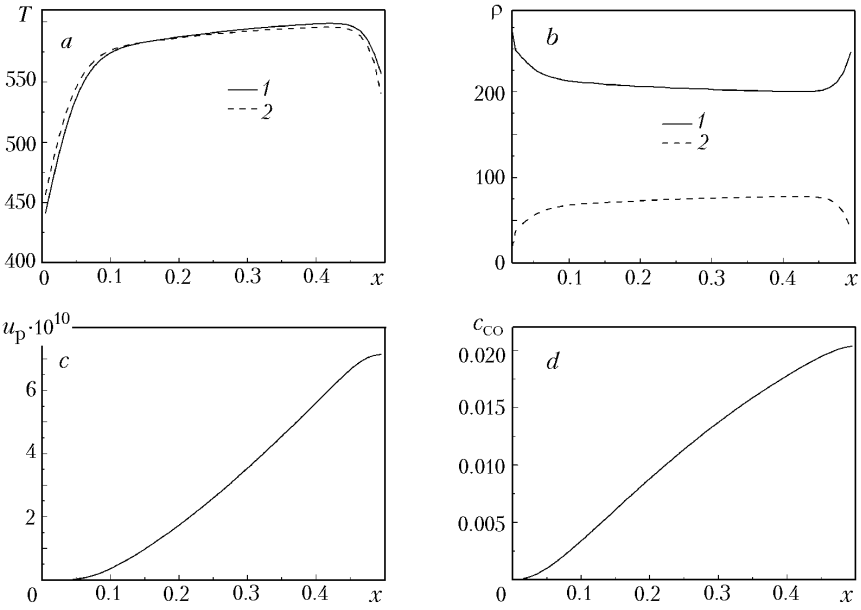

Fig. 5. Low-temperature volume pyrolysis. The profiles of: a) temperatures of the gas T_g (1) and solid T_s (2) phases, b) partial densities in the solid phase of the initial fuel substance ρ_r (1) and carbon ρ_C (2), c) velocity of the particle bed u_p, and d) weight fraction of carbon monoxide c_{CO}. T_g and T_s, K; ρ_r and ρ_C, kg/m^3; u_p, m/sec.

stationary regime is established in this period of time for the gasifier with continuous raw-material feed and ash removal. With an increased flow rate of the blast (Fig. 6, curve 3), the processes of establishment are more rapid and the specific heat content of the producer gas increases.

To determine the basic characteristics of the process, i.e., the heat content of the producer gas and the temperature of the solid phase, we calculate the gasification for air and oxygen-enriched blasts (Figs. 7 and 8.)

Quantitatively the heat content of the producer gas is determined by the content of CO and the chemical equilibrium between CO and CO_2 in the zone of the maximum gasification temperature. Therefore, the heat content of the producer gas is dependent on the production temperature. In turn the temperature of the FC-wave front increases with blast flow rate [5].

Thus, the maximum attainable gasification parameters are determined by a number of factors of a technical nature. The specific flow rate of the blast is primarily limited by the pressure difference in the reactor and the energy consumption by pumping of the blast. Taking into account that the porosity in a complex polydisperse fill can be ~0.3 and the bed thickness in production units (the more so in underground-gasification systems) can be a few meters, the reasonable flow rate of the blast cannot be higher than 0.3–0.5 kg/(m^2·sec). On the other hand, it is known from the theory of FC stability [20] that the higher the rate of pumping of the gas, the higher the rate of growth of perturba-

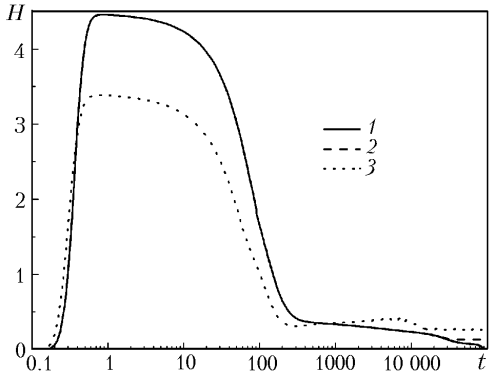

Fig. 6. Variation in the specific heat content of the producer gas with time after switching on the gas producer. Firing is on the source side of the blast feed: 1) closed gasifier with no ash dump; 2 and 3) gasifier with ash dump; 1 and 2) the parameters are standard; 3) φ = 131 kg/(m^2·h), the remaining parameters are standard. *H*, MJ/kg; *t*, sec.

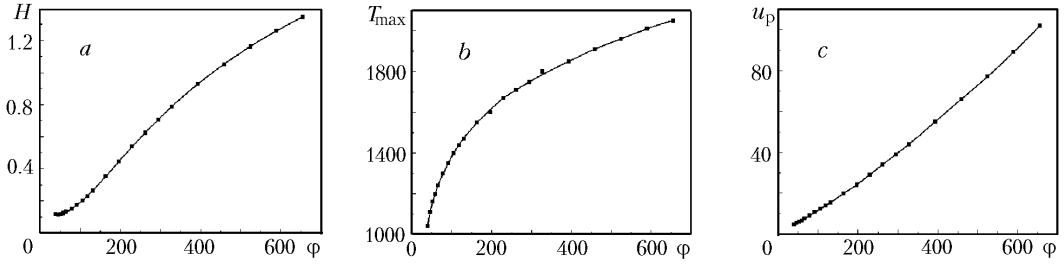

Fig. 7. Characteristics of gasification in the stationary operating regime of a gas producer vs. specific flow rate of an air blast: a) specific heat content of the producer gas; b) maximum temperature of the solid phase; c) rate of feeding of shales. The parameters are standard. *H*, MJ/kg; T_{max}, K; u_p, μm/sec; φ, kg/(m^2·h).

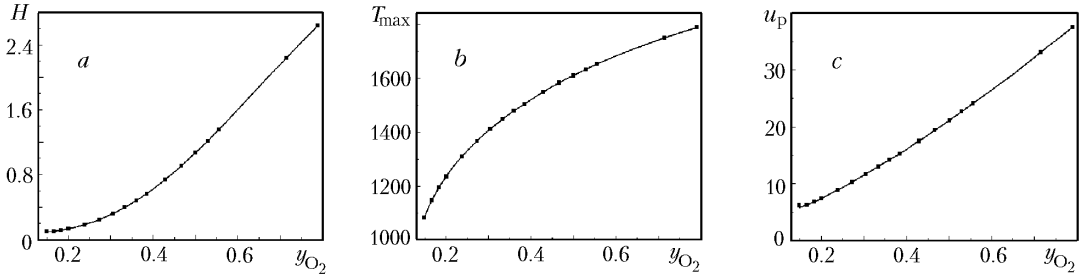

Fig. 8. Characteristics of gasification in the stationary operating regime of a gas producer vs. concentration of oxygen in the blast (the volume flow rate of the blast under normal conditions is standard, the mass flow rate changes in accordance with the blast density). The notation is the same as that in Fig. 7. The parameters are standard. *H*, MJ/kg; T_{max}, K; u_p, μm/sec.

tions and the hazard of breaking deformation of the combustion front. Thus, it is not improbable that it will be necessary to impose additional restrictions on the blast flow rate and thereby on the heat content of the producer gas with the aim of ensuring stable operation of specific technological systems.

The use of the oxygen-enriched blast, as follows from Fig. 8, makes it possible to substantially improve the quality of the producer gas. However, we must take into account the technical difficulties arising in operation with oxygen, the corresponding restrictions of accident prevention, and a special time-limit of works. Taking into account

that the concentration of oxygen on membrane enrichers attains ~45%, and the cost of concentrated oxygen is fairly high, the intensification potential of gasification of shale (Fig. 8) can be evaluated by a level of oxygen concentration in the blast of 45%.

Another problem to be solved in high-temperature gasification of shale is the fusion and sintering of shales and shale ash, which, undoubtedly, degrade the stability and quality of the process, may lead to a discontinuity of the FC front, and requires corresponding manipulations with the raw material and the solid product.

Conclusions. We have analyzed the regimes of filtration combustion and gasification of Belarusian oil shales. We have evaluated the heat content and the temperature parameters of gasification of Belarusian shales in the case of air and oxygen-enriched blast. The upper limit of the heat content of the producer gas can be estimated as 1–1.5 MJ/kg in the case of the air blast and as 3–4 MJ/kg with the oxygen blast. These evaluated parameters can substantially be diminished when the phenomena of instability of the combustion front and gasification appear in a specific technical unit. Furthermore, the high-temperature gasification of shales requires the solution of the problem of sintering of shales and shale ash and manipulation with corresponding products.

This work was carried out within the framework of the "Énergobezopasnost'" State Complex Program of Scientific Research, task 06.

NOTATION

c, weight fraction; c_p, specific heat at constant pressure, J/(kg·K); d, diameter, m; D, diffusion coefficient, m^2/sec; E, activation energy, K; f, volume density of the filtration-resistance force, N/m^3; G, flow rate of the fed gas, m^3/h; g, specific flow rate of the fed gas, $m^3/(m^2 \cdot h)$; h, specific enthalpy, J/kg; H, specific heat content of the producer gas, J/kg; I, diffusion-flux density, kg/(m^2·sec); J, heat-flux density in the gas phase, W/m^2; k_0, permeability coefficient, m^2; k_1, Forchheimer coefficient, m; K, reaction-rate constant, the dimensions are dependent on the reaction order; L, length, m; p, pressure, Pa; P, reaction order; Q, volume heat-release rate, W/m^3; R, rate of formation of the component per unit volume of the gas phase, kg/(m^3·sec); S, specific area of the particle surface, 1/m; s, stoichiometric coefficient; t, time, sec; T, temperature, K; u, velocity, m/sec; V_g, filtration velocity, m/sec; w, rate of expenditure of the component per unit volume of the solid phase, kg/(m^3·sec); x, coordinate, m; Y, molar concentration, mole/m^3; y, molar fraction; z, preexponential factor, the dimensions are dependent on the reaction order; α, coefficient of interphase heat exchange, W/(m^3·K); ε, porosity; λ, thermal conductivity, W/(m·K); μ, coefficient of viscosity, Pa·sec; ρ, density, kg/m^3; φ, specific mass flow rate of the blast, kg/(m^2·h); χ, weight fraction of the carbon yield from the initial fuel substance of shales; ω, emissivity factor of the wall. Subscripts: a, ash; b, firing (burning); b.lt, left-hand boundary of the firing region; b.r, right-hand boundary of the firing region; C, carbon; dis, dispersion; eff, effective; ext, environment, external medium; g, gas phase; h, heterogeneous; i and j, No. of the gas-phase component; k, No. of the reaction; l, No. of the solid-phase component; max, maximum; p, particle; r, initial fuel substance of shales; s, solid phase; 0, initial.

REFERENCES

1. A. N. Shuravin, Resources of oil shales in Belarus, in: *Proc. Int. Sci. Conf.* "*Oil Shales — an Alternative Source of a Fuel and Raw Materials. Fundamental Investigations. Experience and Prospects*" [in Russian], Saratov (2007), pp. 30–31.
2. I. I. Lishtvan (Ed.), *Problems of Complex Use of Oil Shales of the Byelorussian SSR* [in Russian], Nauka i Tekhnika, Minsk (1983).
3. A. F. Gavrilov, Power engineering on the basis of the new technologies of using low-grade fuels, ÉSCO (Electronic J.), No. 10 (2007). (http://www.esco-ecosys.narod.ru/).
4. A. I. Blokhin, G. P. Stel'makh, and K. A. Iorudas, Oil shales for the power engineering and chemistry of Russia, in: *New in the Russian Electrical Power Engineering* (Electronic J.), No. 3 (2001). (http:www.rao-ees/ru/ru/news/news/magazin/).
5. K. V. Dobrego and S. A. Zhdanok, *Physics of Filtration Combustion of Gases* [in Russian], ITMO NAN Belarusi, Minsk (2002).

6. B. V. Kantorovich, *Introduction to the Theory of Combustion and Gasification of a Solid Fuel* [in Russian], Metallurgizdat, Moscow (1960).
7. L. L. Nesterenko, Yu. V. Biryukov, and V. A. Lebedev, *Fundamentals of the Chemistry and Physics of Combustible Fossils* [in Russian], Vishcha Shkola, Kiev (1987).
8. G. N. Makarov and G. D. Kharlampovich (Eds.), *Chemical Technology of Solid Combustible Fossils* [in Russian], Khimiya, Moscow (1986).
9. K. V. Dobrego and I. A. Koznacheev, Regimes of gasification of lean coal layers, *Inzh.-Fiz. Zh.*, **79**, No. 2, 56–61 (2006).
10. S. I. Futko, K. V. Dobrego, E. S. Shmelev, A. V. Suvorov, and S. A. Zhdanok, Thermal recovery of sorbents by filtration combustion, *Combust. Sci. Technol.*, **5**, 883–903 (2007).
11. K. V. Dobrego and I. A. Koznacheev, Generalized volume-averaged filtration-combustion model and its application for calculating carbon gasifiers, *Inzh.-Fiz. Zh.*, **78**, No. 4, 8–14 (2005)
12. R. J. Kee, F. M. Rupley, and J. A. Miller, *The Chemkin Thermodynamic Data Base*, Sandia National Laboratories, Report SAND87-8215B (1990).
13. A. S. Predvoditelev, L. Ya. Khitrin, O. A. Tsukhanova, et al., *Combustion of Carbon* [in Russian], Izd. AN SSSR, Moscow (1949).
14. V. Ya. Basevich, A. A. Belyaev, and S. M. Frolov, Global kinetic mechanisms for calculating turbulent reacting flows. Pt. 1, Basic Chemical Process of Heat Release, *Khim. Fiz.*, **17**, No. 9, 112–128 (1998).
15. K. V. Dobrego, I. M. Kozlov, N. N. Gnezdilov, and V. V. Vasiliev, *2DBurner — Software Package for Gas Filtration Combustion Systems Simulation and Gas Non-steady Flames Simulation*, Preprint No. 1 of the Heat and Mass Transfer Institute, Minsk (2004).
16. K. V. Dobrego, I. M. Kozlov, and N. N. Gnezdilov, Model and methods of 2D simulation of filtration combustion reactors with arbitrary chemical kinetics, in: *Proc. 9th Int. Conf. on Numerical Combustion*, April 7–10, Sorrento, Italy (2002), pp. 317–319.
17. R. W. Hockney and J. W. Eastwood, *Computer Simulation Using Particles*, McGraw-Hill Inc., New York (1981).
18. A. Harten, High-resolution schemes for hyperbolic conservation laws, *J. Comput. Phys.*, **49**, 357–393 (1983).
19. K. V. Dobrego, N. N. Gnezdilov, I. M. Kozlov, and E. S. Shmelev, Numerical study and optimization of the porous media VOC oxidizer with electric heating elements, *Int. J. Heat Mass Transfer*, **49**, 5062–5069 (2006).
20. K. V. Dobrego, I. M. Kozlov, V. I. Bubnovich, and C. E. Rosas, Dynamics of filtration combustion front perturbation in the tubular porous media burner, *Int. J. Heat Mass Transfer*, **46**, 3279–3289 (2003).